

Generation of Pure Bulk Valley Current in Graphene

Yongjin Jiang,^{1,2,*} Tony Low,³ Kai Chang,^{4,2,†} Mikhail I. Katsnelson,⁵ and Francisco Guinea⁶

¹Center for Statistical and Theoretical Condensed Matter Physics and Department of Physics,
Zhejiang Normal University, Jinhua 321004, People's Republic of China

²Beijing Computational Science Research Center, Beijing 100084, People's Republic of China

³IBM T.J. Watson Research Center, Yorktown Heights, New York 10598, USA

⁴SKLSM, Institute of Semiconductors, Chinese Academy of Sciences, P.O. Box 912, Beijing 100083, People's Republic of China

⁵Radboud University Nijmegen, Institute for Molecules and Materials, Heyendaalseweg 135, 6525AJ Nijmegen, The Netherlands

⁶Instituto de Ciencia de Materiales de Madrid, CSIC, Sor Juana Inés de la Cruz 3, 28049 Madrid, Spain

(Received 6 September 2012; published 23 January 2013)

The generation of valley current is a fundamental goal in graphene valleytronics but no practical ways of its realization are known yet. We propose a workable scheme for the generation of bulk valley current in a graphene mechanical resonator through adiabatic cyclic deformations of the strains and a chemical potential in the suspended region. The accompanied strain gauge fields can break the spatial mirror symmetry of the problem within each of the two inequivalent valleys, leading to a finite valley current due to quantum pumping. An all-electrical measurement configuration is designed to detect the novel state with pure bulk valley currents.

DOI: 10.1103/PhysRevLett.110.046601

PACS numbers: 72.80.Vp, 73.63.-b, 85.85.+j

Apart from pseudospin (chirality), charge carriers in graphene are also characterized by the valley index (sometimes called isospin) originating from the existence of two conical (Dirac) points per Brillouin zone [1]. A valley polarized state requires the absence of time reversal symmetry, as the two valleys are related by this symmetry.

Motivated by the growing field of spintronics [2,3], it has been proposed that manipulation of the valley index may open a new way to transmit information through graphene, and different manipulation schemes were proposed [4–12]. After the initial enthusiasm, interest in “valleytronics” declined somehow, as it was soon realized that a valley polarized current will be degraded by intervalley scattering induced by atomic scale disorder [1], making the maintenance of valley polarized states difficult. In addition, a number of proposals were based on the spatial separation of valley currents at zigzag edges [4], which requires well-defined edge orientation and that the edge currents are free of short range scattering.

We present a new scheme to induce valley polarized currents in graphene which avoids some of the pitfalls of previous proposals. The breaking of time reversal symmetry is achieved by means of time dependent fields, instead of a magnetic field. The induction of valley polarization by ac fields has been proven in MoS₂ [13] as well as in (111)-oriented silicon metal-oxide-semiconductor field-effect transistors [14] where optical radiation was used in order to excite valley polarized charge carriers. As in these experiments, the scheme discussed below generates valley currents throughout the entire system. However, the ac driving force in our proposal is due to mechanical vibrations of a nanoelectrical-mechanical system (NEMS [15–18]), as illustrated in Fig. 1(a).

We employ a continuum-medium description of graphene with the Dirac Hamiltonian,

$$\mathcal{H}^{\pm}(\vec{k}, \vec{\mathcal{A}}) = \hbar v_f [\pm(k_x \mp \mathcal{A}_x)\sigma_x + (k_y \mp \mathcal{A}_y)\sigma_y] + \mu \mathbb{1}_2, \quad (1)$$

where $+$ ($-$) denotes the K (K') valley index, v_f is the Fermi velocity, and μ is the chemical potential. $\vec{\mathcal{A}}(\vec{r})$ is an effective gauge field describing the modifications to the hopping amplitudes induced by the strain fields $u_{ij}(\vec{r})$ [19,20], and has opposite signs at the two valleys as required by time-reversal symmetry. We described the deformation of the suspended region, i.e., $-\frac{L}{2} < y < \frac{L}{2}$, with a simple uniaxial strain given by $u_{yy} = u$ and $u_{xx} = u_{xy} = 0$. It will be shown below that for arbitrary crystallographic orientation θ [see Fig. 1(b)], $\vec{\mathcal{A}}(\vec{r})$ in the suspended region is given by the expression

$$\vec{\mathcal{A}}(\vec{r}) = \frac{\beta \kappa u}{a} (-\cos 3\theta, \sin 3\theta), \quad (2)$$

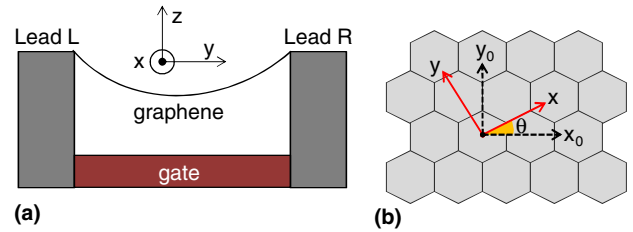


FIG. 1 (color online). Illustration and definitions of the (a) graphene based NEMS device and (b) crystallographic coordinate systems used in the Letter.

where $\beta \approx 2$ is the electron Gruneisen parameter and $\kappa \approx \frac{1}{3}$ is a parameter related to graphene's elastic property as described in Ref. [19]. $a \approx 1.4 \text{ \AA}$ is the interatomic distance. Adiabatic cyclic variations of the internal parameters, such as deformations in the strains (u) and chemical potential (μ) in the suspended region, over a work cycle can constitute a scheme for adiabatic quantum pumping [21,22] (for the general theory of quantum pumping, see Refs. [23,24]). For the charge pumping one needs to break the spatial mirror symmetry, e.g., making the right and left leads different (e.g., by different doping) [24]. Here we will demonstrate that for the case of *symmetric* leads the *valley* current through the system is, in general, nonzero. In this case, the pumping current through each channel will be shown to follow the general relation (with periodic boundary condition along the transversal x direction),

$$I_{L(R)}^{\text{pump},K}(k_x, \theta) = -I_{L(R)}^{\text{pump},K'}(-k_x, \theta) \neq 0 \quad \text{if } \theta \neq n\frac{\pi}{3}, \quad (3)$$

where the subscript L(R) refers to the left (right) lead ($I_{L(R)}$ is defined positive when the current flows out of the device). Equation (3) represents the central result of our Letter, and embodies the intrinsic symmetry of valley pumping in graphene NEMSs, as we will show later. Below, we present detailed derivations leading to Eq. (3) and discuss the physical consequences that follow, such as the generation of pure bulk valley current and its possible experimental detection.

We start by considering the case $\theta = 0$, where the trench is directed along the zigzag direction [see the (x_0, y_0) coordinate system shown in Fig. 1(b)]. In this case, the Hamiltonian has the form of Eq. (1) and the pseudomagnetic vector potential reads

$$\mathcal{A}_x = \frac{\beta\kappa}{a}(u_{xx} - u_{yy}), \quad \mathcal{A}_y = -\frac{2\beta\kappa}{a}u_{xy}. \quad (4)$$

For arbitrary orientation, i.e., $\theta \neq 0$, Eqs. (1) and (4) have to be recast in the new coordinate frame (x, y) . The two coordinate systems are related by

$$\begin{pmatrix} x \\ y \end{pmatrix} = \mathcal{R} \begin{pmatrix} x_0 \\ y_0 \end{pmatrix}, \quad \mathcal{R} = \begin{pmatrix} \cos \theta & \sin \theta \\ -\sin \theta & \cos \theta \end{pmatrix}. \quad (5)$$

The wave vector \vec{k} transforms in the same way as \vec{r} such that $\vec{k} \cdot \vec{r}$ is a rotational invariant quantity. The strain field is defined as $u_{ij} = \frac{1}{2}(\frac{\partial u_j}{\partial x_i} + \frac{\partial u_i}{\partial x_j})$, which is a symmetric tensor of rank two. Hereafter we use the subscript or superscript 0 to denote physical quantities in the original frame (x_0, y_0) . Thus, we have $\vec{k}_0 = R^{-1}\vec{k}$ and

$$\begin{aligned} u_{xx}^0 - u_{yy}^0 &= \cos 2\theta(u_{xx} - u_{yy}) - 2\sin 2\theta u_{xy}, \\ u_{xy}^0 &= \frac{1}{2}\sin 2\theta(u_{xx} - u_{yy}) + \cos 2\theta u_{xy}. \end{aligned} \quad (6)$$

By using the new coordinates in the Dirac Hamiltonian, we can transform it to the rotated frame,

$$\mathcal{H}^\pm(\vec{k}, \vec{\mathcal{A}}) = \hbar v_f \left(\frac{\mu/\hbar v_f}{e^{\pm i\theta}[(\pm k_x + ik_y) \mp (\pm \mathcal{A}_x + i\mathcal{A}_y)]} \right), \quad (7)$$

where we have defined the pseudomagnetic field $\vec{\mathcal{A}}$ in the rotated frame as [25]

$$\begin{pmatrix} \mathcal{A}_x \\ \mathcal{A}_y \end{pmatrix} = \mathcal{R}(3\theta) \begin{pmatrix} \frac{\beta\kappa}{a}(u_{xx} - u_{yy}) \\ -\frac{2\beta\kappa}{a}u_{xy} \end{pmatrix}. \quad (8)$$

Equations (7) and (8) constitute the continuum-medium description of strained graphene in an arbitrarily rotated frame. Here, two comments follow about this general form. First, if we perform the gauge transformation of the wave function on the B sublattice $\psi_B^{\pm K} \rightarrow \psi_B^{\pm K} e^{\pm i\theta}$, the Dirac Hamiltonian can be made explicitly invariant [i.e., Eq. (1)] under rotation. Thus, we can simply drop the factor $e^{\pm i\theta}$ in Eq. (7) in the subsequent discussion. Second, from the definition for pseudomagnetic field, it is obvious that the form is of $2\pi/3$ periodic in θ , which reflects the trigonal symmetry of the underlying honeycomb lattice.

Next, we describe the quantum pumping problem based on graphene NEMSs [22,26]. As discussed above, the derived Hamiltonian given by Eq. (7) is physically

equivalent to Eq. (1). Suppose that between $-\frac{L}{2} < y < \frac{L}{2}$, the system has uniaxial strain $u_{yy} = u$ and $u_{xx} = u_{xy} = 0$; hence, Eq. (8) is reduced to

$$(\mathcal{A}_x, \mathcal{A}_y)(\vec{r}) = \begin{cases} 0, & |y| > \frac{L}{2} \\ \left(\frac{\beta\kappa u}{a}\right)(-\cos 3\theta, \sin 3\theta), & |y| \leq \frac{L}{2} \end{cases} \quad (9)$$

with the expression given in Eq. (2) for the suspended region. In the following, assuming a particular geometry (the width $W \gg L$), the x direction is treated as translationally invariant. From Eqs. (7) and (9), one can easily see that

$$\mathcal{H}^+(k_x, k_y, \vec{\mathcal{A}}, \theta) = \mathcal{H}^-(k_x, k_y, \vec{\mathcal{A}}, -\theta). \quad (10)$$

We can call such combined symmetry the *crystalline-angle-combined mirror symmetry* in the continuum-medium model. It turns out that such combined symmetry has a significant consequence on the relation of pumping currents in each valley, i.e., Eq. (3), as will be elaborated further.

Due to the mentioned symmetry, we may focus only on the K Dirac cone, whose Hamiltonian has the following form for the different regions (i.e., $i = L, R$, and G denote $y < -\frac{L}{2}$, $y > \frac{L}{2}$, and $|y| \leq \frac{L}{2}$, respectively):

$$\mathcal{H}_i^+(\vec{k}, \vec{\mathcal{A}}) = \hbar v_f \begin{pmatrix} \epsilon_i / \hbar v_f & (\tilde{k}_x - i\tilde{k}_y)_i \\ (\tilde{k}_x + i\tilde{k}_y)_i & \epsilon_i / \hbar v_f \end{pmatrix}, \quad (11)$$

where we have defined $(\tilde{k}_x, \tilde{k}_y)_i = (k_x - \mathcal{A}_x, k_y - \mathcal{A}_y)_i$. In this Letter, we consider mainly the symmetric case $\epsilon_L = \epsilon_R \neq \epsilon_G$.

The eigenenergies and eigenstates of the Hamiltonian in Eq. (11) read

$$E_{i,s}(\vec{k}) = \epsilon_i + s\hbar v_f \sqrt{\tilde{k}_x^2 + \tilde{k}_y^2}, \quad (12)$$

$$\psi_{i,s}(\vec{k}) = e^{i(k_x x + k_y y)} \begin{pmatrix} 1 \\ \frac{\hbar v_f (\tilde{k}_x + i\tilde{k}_y)_i}{E_{i,s} - \epsilon_i} \end{pmatrix},$$

where $s = \pm 1$ refers to the electron or hole band, respectively. Due to translational invariance in x direction, k_x is the same in all three regions. We consider now the equilibrium situation where all three regions can be described by a common chemical potential μ . Obviously, \tilde{k}_{x_i} is always real since k_x is real. Then, $\tilde{k}_{y_i} = \pm \sqrt{k_{f_i}^2 - \tilde{k}_{x_i}^2}$, where $k_{f_i} = \frac{\mu - \epsilon_i}{\hbar v_f}$ and the \pm sign is selected to give the correct sign in the group velocity, depending on whether it is an incident, transmitted, or reflected wave. Note that \tilde{k}_y can be purely imaginary representing evanescent waves in the central region.

It is straightforward to calculate the scattering matrix for our device. Without loss of generality, we can focus on the case with the electron doping ($\mu - \epsilon_L > 0$) in the leads. The scattering coefficients are calculated to be

$$r_d = e^{-ik_{yL}L} \frac{C_2(d) + C_3(d)}{C_1(d)}, \quad (13)$$

$$t_d = e^{-ik_{yL}L} \frac{-4 \sin \varphi_L \sin \varphi_G e^{iA_y L d}}{C_1(d)},$$

where r_d and t_d are the reflection and transmission coefficients with $d = 1(-1)$ corresponding to the cases with incident waves from $y = -\infty$ (left lead) and $y = \infty$ (right lead), respectively; φ_L and φ_G are defined through

$$e^{\pm i\varphi_L} = \frac{k_x \pm ik_{yL}d}{k_{f_L}}, \quad e^{\pm i\varphi_G} = \frac{\tilde{k}_{xG} \pm i\tilde{k}_{yG}}{k_{f_G}}. \quad (14)$$

The $C_i(d)$ in Eq. (13) are defined as

$$C_1(d) = 4i \sin(\tilde{k}_{yG} L d) (1 - \cos \varphi_L \cos \varphi_G) - 4 \cos(\tilde{k}_{yG} L d) \sin \varphi_L \sin \varphi_G, \quad (15)$$

$$C_2(d) = -2i(1 + e^{2i\varphi_L}) \sin(\tilde{k}_{yG} L d),$$

$$C_3(d) = 2ie^{i\varphi_L} [\sin(\tilde{k}_{yG} L d + \varphi_G) + \sin(\tilde{k}_{yG} L d - \varphi_G)].$$

Symmetries related with t_d and r_d .—Next, we discuss symmetry properties of the scattering amplitudes. First, we note that $\varphi_G(d) = \varphi_G(-d)$, $\varphi_L(d) = -\varphi_L(-d)$ and they are independent of the sign of θ . Then, we can obtain the relations satisfied by C_i 's: $C_1(d) = -C_1(-d)$, $C_{2,3}(-d)^* = C_{2,3}(d)$. Based on these relations and the odd parity of $\mathcal{A}_y(\theta)$, we arrive at

$$t_d(k_x, \theta) = t_{-d}(k_x, -\theta), \quad r_d(k_x, \theta) = r_d(k_x, -\theta). \quad (16)$$

Symmetry of pumped valley-dependent current.—According to the adiabatic pumping theory [23] and the symmetry relations satisfied by r_d and t_d , we obtain the following relation for the pumping current $I_L^{\text{pump},K}(k_x, \theta)$ for K valley:

$$I_L^{\text{pump},K}(k_x, \theta) - I_R^{\text{pump},K}(k_x, -\theta) = \frac{ie\omega}{4\pi^2} \int_0^{2\pi/\omega} ds \left[\frac{dr_1(\theta)}{ds} r_1(\theta)^* - \frac{dr_{-1}(\theta)}{ds} r_{-1}(\theta)^* \right], \quad (17)$$

where we've used s as the time symbol to avoid confusion with the transmission coefficient. Now, using the symmetry relations satisfied by C_i 's and the fact that the common complex factors for C_2 and C_3 , i.e., $ie^{i\varphi_L}$, are independent of time [see Eq. (19) for typical time dependence of pumping parameters for graphene NEMS], we can simply prove that the integrand in Eq. (17) is zero. By further taking into account the current conservation condition [$I_L^{\text{pump},K}(k_x, -\theta) + I_R^{\text{pump},K}(k_x, -\theta) = 0$] and the symmetry relation guaranteed by Eq. (10) [i.e., $I_L^{\text{pump},K'}(-k_x, \theta) = I_L^{\text{pump},K}(k_x, -\theta)$], we arrive at the first part of Eq. (3), the relation for pumped valley-dependent current, which is the central result of this Letter. The above derivation based on the explicit solution of scattering amplitudes demonstrates the usefulness of the generic crystalline-angle-combined mirror symmetry of the suspended graphene under uniaxial strain. Later we will show that Eq. (3) and its consequences are consistent with the inversion symmetry of the whole system.

Next, we discuss some direct consequences of Eq. (3). By integrating out the transversal wave vector k_x , we can get the following relation:

$$I_{L(R)}^{\text{pump},K}(\theta) = -I_{L(R)}^{\text{pump},K'}(\theta). \quad (18)$$

Equation (18) means that the total pumping current at a given lead is opposite for different valleys. Thus, the total charge current is exactly zero. This situation is analogous to the pure spin current generation in spintronics [27,28]; thus, we call this effect pure valley current generation. In summary, we have shown that the application of an alternating backgate voltage to graphene NEMSs can induce a pure valley current via adiabatic pumping. In adiabatic pumping theory, there are two necessary conditions for a finite charge pumping effect, i.e., time reversal symmetry

breaking and mirror symmetry breaking of the left or right lead [24]. The above derivations show that the valley pumping effect can be realized in a *seemingly* symmetric two-terminal geometry with identical leads. However, the mirror symmetry of the system (i.e., $y \rightarrow -y$) has actually been broken for each valley when $\theta \neq \frac{n\pi}{3}$. Such symmetry breaking is embodied in the continuum theory through a nonzero \mathcal{A}_y component. This constitutes the second part of Eq. (3). For a more quantitative understanding, we present some numerical results of $I_L^{\text{pump},K}(\theta)$ (in terms of the pumped charge per cycle) for the K valley in Fig. 2 using some typical experimental parameters, as discussed below.

As stated above, the strain (u) and Dirac potential (ϵ_G) in the suspended region are modulated by the ac backgate voltage. Near resonance, they differ by a phase difference ϕ with a typical time dependence given by (with conventional time symbol t) [22]

$$\begin{aligned}\epsilon_G &= \epsilon_{G0}[1 + \delta\epsilon \cos(\omega t)]^{1/2}, \\ \vec{\mathcal{A}} &= \vec{\mathcal{A}}_0[1 + \delta\mathcal{A} \cos(\omega t + \phi)]^2.\end{aligned}\quad (19)$$

Assuming typical numbers for the static part $\epsilon_{G0} = \epsilon_L = 0.3$ eV, $\vec{\mathcal{A}}_0 = 0.02k_f(\cos 3\theta, -\sin 3\theta)$, and the oscillating amplitude $\delta\epsilon = \delta\mathcal{A} = 0.2$, we calculated the pumped charge per cycle $Q_c^K(\theta)$ for K valley, as shown in Fig. 2. By definition, the pumping current $I_L^{\text{pump},K}(\theta) = e\omega Q_c^K(\theta)/2\pi$. Our calculation indicates a nearly linear scaling (not shown) of the pumping effect on length L of the NEMSs, which is similar to the results in Ref. [22]. As explicitly shown, the maximum pumping effect is reached for the crystallographic angles corresponding to the armchair-type x axis ($\theta = \pi/2 + n\pi/3$, $n \in \mathbb{Z}$) while it is zero at the zigzag-type x axis ($\theta = n\pi/3$, $n \in \mathbb{Z}$). The

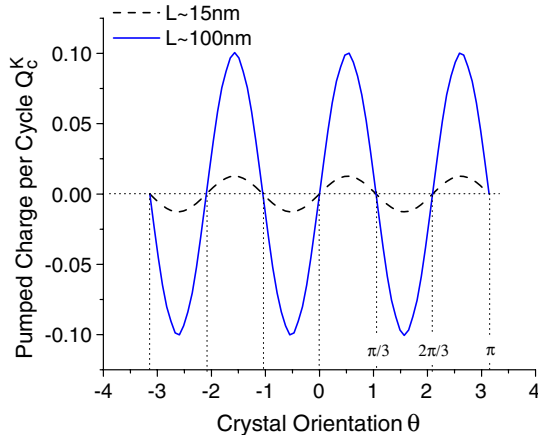


FIG. 2 (color online). The pumped charge per cycle of the K valley, denoted as Q_c^K . The valley current can be obtained by $e\omega Q_c^K/2\pi$. The width is fixed to be $5000a$ (≈ 700 nm), calculated for two different lengths as indicated. We fixed the phase difference of the driving parameters $\phi = \pi/2$ and take $|\vec{\mathcal{A}}_{av}|/k_f \approx 0.002$, which amounts to a strain $u \approx 1.75 \times 10^{-4}$.

periodicity $2\pi/3$ with θ is easily seen. The valley current can be defined as $I^{\text{pump},v}(\theta) = I^{\text{pump},K}(\theta) - I^{\text{pump},K'}(\theta)$, which is simply twice the value of $I^{\text{pump},K}(\theta)$. For the typical resonance frequency of $\omega \approx 10$ MHz [17] to 0.16 GHz [18], we arrive at numerical estimates $I^{\text{pump},v} \approx 0.1$ – 10 pA/ μm , a quantity measurable in experiment. Furthermore, the signal can be amplified by (i) increasing the area of suspended graphene part (the signal is roughly proportional to both length and width in the theoretical model we considered) and (ii) tuning the amplitude of the ac voltage of the backgate to increase the oscillation magnitude of strain or chemical potential.

The possibility of pure bulk valley current in this simple pumping scenario looks very promising. The problem is how to probe the valley current. Here we propose an all-electrical measurement as shown in Fig. 3 (note the voltage contacts are patterned on the supporting leads, instead of on the suspended region). From Eq. (3), we can infer that the charge current pertaining to carriers from the valley K not only has an opposite longitudinal component with respect to the charge carriers from the valley K' , but also their transversal velocities are opposite. As pictorially shown in Fig. 3, we expect charges accumulating on opposite edges on the two sides of the NEMS. Based on this observation, we predict that the resultant Hall voltage on the left lead has the opposite sign of that on the right lead, i.e., $\text{sgn}(V_{12}/V_{34}) = -1$, which is the characteristic feature of the bulk valley current flow.

The above picture can be made more quantitative. Because k_x , like charge, is a conserved quantum number in our pumping scenario, we can introduce a quantity, *valley-dependent pumping Hall current*, which can be calculated as $I_{L(R)}^{\text{Hall},K}(\theta) = \sum_{k_x} I_{L(R)}^{\text{pump},K}(k_x, \theta) \frac{k_x}{k_y}$. This Hall current accompanying the pure bulk valley current can be viewed as a result of the effective pumping force, instead of the usual Lorentz force due to a magnetic field. From Eq. (3) and the particle conservation law for each k_x channel, we can obtain

$$I_{L(R)}^{\text{Hall},K}(\theta) = I_{L(R)}^{\text{Hall},K'}(\theta) = -I_{R(L)}^{\text{Hall},K}(\theta). \quad (20)$$

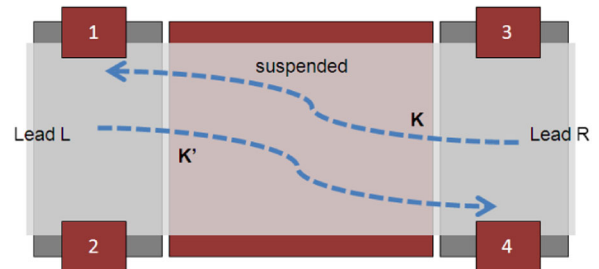


FIG. 3 (color online). Sketch of the pumping generation of pure valley current and an all-electrical detection scheme. The Hall voltage difference $V_{12} = V_1 - V_2$ and $V_{34} = V_3 - V_4$ across the NEMS is predicted to bear the opposite sign due to the flow of pure valley current.

Such Hall current on different leads can result in the opposite Hall voltage. Thus the existence of pure valley currents possibly can be detected in the leads by means of nonlocal multiterminal measurements [29]. Finally, it's worthy to point out that such a hall current pattern is a reasonable consequence of inversion symmetry and time reversal symmetry breaking of the system.

Our discussion above is restricted to the case with symmetrical leads. It is straightforward to extend our study to the more general case with differently doped leads. In the general situation, the current is not purely valley current, i.e., $I_{L(R)}^{\text{pump},K}(\theta) \neq -I_{L(R)}^{\text{pump},K'}(\theta)$; thus, the charge pumping current is finite.

To conclude, we have shown that through pumping induced by mechanical vibrations bulk valley polarized currents can be generated in graphene leads connecting the graphene resonator with the trench directed at a general crystallographic angle. We have demonstrated that the generated current is purely a valley current (with zero net charge pumping current) in the setup with the same doping rate in the graphene leads. Together with an all-electrical measurement scheme, our proposal opens a new direction of exploiting the valley degree of freedom, thus pushing graphene-based valleytronics a step forward toward real applications.

Y.J. and K.C. acknowledge the support from the National Natural Science Foundation of China [under Grants No. 11004174 (Y.J.) and No. 10934007 (K.C.)]. Y.J. is also supported by the Program for Innovative Research Team in Zhejiang Normal University. K.C. is also supported by the National Basic Research Program of China (973 Program) under Grant No. 2011CB922204. T.L. also acknowledges partial support from NRI-INDEX. M.I.K. acknowledges financial support from FOM, Netherlands. F.G. acknowledges financial support from Spanish MICINN (Grants No. FIS2008-00124, No. FIS2011-23713, and No. CONSOLIDER CSD2007-00010), and ERC, Grant No. 290846.

*jyj@zjnu.cn

†kchang@semi.ac.cn

- [1] A. H. Castro Neto, F. Guinea, N. M. R. Peres, K. S. Novoselov, and A. K. Geim, *Rev. Mod. Phys.* **81**, 109 (2009); N. M. R. Peres, *Rev. Mod. Phys.* **82**, 2673 (2010); S. Das Sarma, S. Adam, E. H. Hwang, and E. Rossi, *Rev. Mod. Phys.* **83**, 407 (2011); M. I. Katsnelson, *Graphene: Carbon in Two Dimensions* (Cambridge University Press, Cambridge, England, 2012).
- [2] I. Zutic, J. Fabian, and S. Das Sarma, *Rev. Mod. Phys.* **76**, 323 (2004);
- [3] S. A. Tarasenko and E. L. Ivchenko, *JETP Lett.* **81**, 231 (2005).
- [4] A. Rycerz, J. Tworzydło, and C. W. J. Beenakker, *Nat. Phys.* **3**, 172 (2007).
- [5] D. Xiao, W. Yao, and Q. Niu, *Phys. Rev. Lett.* **99**, 236809 (2007).
- [6] I. Martin, Y. M. Blanter, and A. F. Morpurgo, *Phys. Rev. Lett.* **100**, 036804 (2008).
- [7] J. M. Pereira, F. M. Peeters, R. N. Costa Filho, and G. A. Farias, *J. Phys. Condens. Matter* **21**, 045301 (2009).
- [8] Z. Wu, F. Zhai, F. M. Peeters, H. Q. Xu, and K. Chang, *Phys. Rev. Lett.* **106**, 176802 (2011).
- [9] J. L. Garcia-Pomar, A. Cortija, and M. Nieto-Vesperinas, *Phys. Rev. Lett.* **100**, 236801 (2008).
- [10] H. Schomerus, *Phys. Rev. B* **82**, 165409 (2010).
- [11] T. Low and F. Guinea, *Nano Lett.* **10**, 3551 (2010).
- [12] L. E. Golub, S. A. Tarasenko, M. V. Entin, and L. I. Magarill, *Phys. Rev. B* **84**, 195408 (2011).
- [13] G. Sallen *et al.*, *Phys. Rev. B* **86**, 081301(R) (2012); H. Zeng, J. Dai, W. Yao, D. Xiao, and X. Cui, *Nat. Nanotechnol.* **7**, 490 (2012); K. F. Mak, K. He, J. Shan, and T. F. Heinz, *Nat. Nanotechnol.* **7**, 494 (2012).
- [14] J. Karch, S. Tarasenko, E. Ivchenko, J. Kamann, P. Olbrich, M. Utz, Z. Kvon, and S. Ganichev, *Phys. Rev. B* **83**, 121312(R) (2011).
- [15] J. S. Bunch, A. M. van der Zande, S. S. Verbridge, I. W. Frank, D. M. Tanenbaum, J. M. Parpia, H. G. Craighead, and P. L. McEuen, *Science* **315**, 490 (2007).
- [16] D. Garcia-Sanchez, A. M. van der Zande, B. L. A. San Paulo, P. L. McEuen, and A. Bachtold, *Nano Lett.* **8**, 1399 (2008).
- [17] C. Chen, S. Rosenblatt, K. I. Bolotin, W. Kalb, P. Kim, I. Kymissis, H. L. Stormer, T. F. Heinz, and J. Hone, *Nat. Nanotechnol.* **4**, 861 (2009).
- [18] A. Eichler, J. Moser, J. Chaste, M. Zdrojek, I. Wilson-Rae, and A. Bachtold, *Nat. Nanotechnol.* **6**, 339 (2011).
- [19] H. Suzuura and T. Ando, *Phys. Rev. B* **65**, 235412 (2002).
- [20] M. A. H. Vozmediano, M. I. Katsnelson, and F. Guinea, *Phys. Rep.* **496**, 109 (2010).
- [21] E. Prada, P. San-Jose, and H. Schomerus, *Phys. Rev. B* **80**, 245414 (2009).
- [22] T. Low, Y. Jiang, M. Katsnelson, and F. Guinea, *Nano Lett.* **12**, 850 (2012).
- [23] P. W. Brouwer, *Phys. Rev. B* **58**, R10135 (1998).
- [24] M. Moskalets and M. Buttiker, *Phys. Rev. B* **66**, 205320 (2002).
- [25] F. Zhai, X. Zhao, K. Chang, and H. Q. Xu, *Phys. Rev. B* **82**, 115442 (2010).
- [26] M. M. Fogler, F. Guinea, and M. I. Katsnelson, *Phys. Rev. Lett.* **101**, 226804 (2008).
- [27] Koki Takanashi, *Jpn. J. Appl. Phys.* **49**, 110001 (2010).
- [28] Y. Avishai, D. Cohen, and N. Nagaosa, *Phys. Rev. Lett.* **104**, 196601 (2010).
- [29] D. A. Abanin, S. V. Mozorov, L. A. Ponomarenko, A. S. Mayorov, M. I. Katsnelson, K. Watanabe, T. Taniguchi, K. S. Novoselov, and A. K. Geim, *Science* **332**, 328 (2011).